



Ultra-fast tunable optoelectronic 2-to-4 binary decoder using graphene-coated silica rods in photonic crystal ring resonators

Salah Naghizade¹ · Azadeh Didari-Bader² · Hamed Saghaei^{3,4}

Received: 28 July 2022 / Accepted: 31 August 2022 / Published online: 27 September 2022
© The Author(s), under exclusive licence to Springer Science+Business Media, LLC, part of Springer Nature 2022

Abstract

Fast and compact optoelectronic devices are highly sought after for applications in high-speed signal processing in optical communication networks. One approach to realizing such devices is through all-optical digital logic circuits. One of the main building blocks of such circuits is a decoder. In this work, we present a novel design for a tunable optoelectronic 2-to-4 binary decoder. The presented structure is realized by utilizing three photonic crystal (PhC) ring resonators. Each PhC ring resonator is formed by silicon rods encircled by silica (SiO₂) rods coated with graphene nanoshells (GNSs). By adjusting the chemical potential of GNS with a proper gate voltage, we can tune the desired PhC resonant mode. The fundamental PhC microstructure's photonic band structure is analyzed by using the plane wave expansion method. Furthermore, the finite-difference time-domain technique is used to solve Maxwell's equations and analyze the light propagation within the structure. Our numerical results reveal that 0.8 ps and 0.3 ps are the maximum rise and fall times for the final structure, respectively and the total size of this device is 850 μm². Due to the short rise and fall times and its size which are among very important features in high-speed systems, the proposed design could be utilized for high-speed signal processing systems in miniaturized optical communication network devices.

Keywords Photonic crystal · Optoelectronic decoder · Graphene-coated silica rods · Chemical potential · Light propagation · Finite-difference time-domain method

✉ Hamed Saghaei
h.saghaei@iaushk.ac.ir

¹ Young Researchers and Elite Club, Tabriz Branch, Islamic Azad University, Tabriz, Iran

² Dale E. and Sarah Ann Fowler School of Engineering, Chapman University, Orange, CA, USA

³ Department of Electrical Engineering, Shahrekord Branch, Islamic Azad University, Shahrekord, Iran

⁴ Energy Research Center, Shahrekord Branch, Islamic Azad University, Shahrekord, Iran

1 Introduction

Optoelectronics which is a branch of photonics is the technology of light detection and emission in electronic devices (Sun et al. 2016). These devices have a broad range of applications such as in sensing, solar cells, fast signal processing, and optical and electronic converters (Bao and Loh 2012), to name a few. With the ever-growing advancements in technology, the demand for fast and compact optical devices has increased greatly in the past decades. Therefore, optoelectronic devices that are capable of addressing these demands are highly sought after. Among these are fully optical signal processing devices whose main body is made of logic circuits (Rahmani and Mehdizadeh 2018; Saghaei et al. 2017; Sharifi et al. 2016; Wabnitz and Eggleton 2015). These devices incorporate logic gates (Cheraghi et al. 2018; Chhipa et al. 2021; Jiang et al. 2015; Liu and Ouyang 2008; Maleki et al. 2020; Sani et al. 2020; Vali-Nasab et al. 2019), combinational logic circuits, and full-adders to realize high-speed signal processing. To this end, Photonic Crystals (PhCs) have become an alternative approach in the design of all-optical devices (Alipour-Banaei et al. 2015b). Due to their photonic bandgap, PhCs allow for selective and tunable emission paths in waveguides (Yablonovitch 1993). In recent years, an extensive amount of research has been done on the material and design selection of PhCs to achieve application-specific solutions.

Research on material selection such as GaAs, InP, and Si on SiO₂ has gained a lot of attention in integrated photonic circuits (Calizo et al. 2007; Danaie and Kaatuzian 2011; Roelkens et al. 2005). Further research on SiO₂ as the substrate has shown advantageous functionalities such as very low loss and low thermal sensitivity within the near-infrared (Ebnali-Heidari et al. 2014, 2012; Song and Williams 1993). Further, the role of structural design in photonic crystal ring resonators (PCRR) in realizing compact optical devices was investigated (Alipour-Banaei et al. 2015a; Mehdizadeh et al. 2016; Rakhshani and Mansouri-Birjandi 2014). These devices can be spectrally tailored based on their rod's refractive index, the structures' lattice constant, and the design parameters of the rod such as radius, and height (Farmani et al. 2020; Mansouri-Birjandi et al. 2016; Tavousi et al. 2017). Furthermore, the spectrally selective resonances in PCRR devices can be tuned to create either a blue or red shift based on the desired application (Naghizade and Saghaei 2021). The use of PCRRs in PhCs as optical filters have been investigated for various applications such as optical filters (Alipour-Banaei et al. 2014; Guo et al. 2019; Naghizade and Saghaei 2020a; Rakhshani and Mansouri-Birjandi 2013), logic gates (Andalib and Granpayeh 2009; Hussein et al. 2018; Younis et al. 2014), Optical encoders-decoders (Haddadan et al. 2020; Maleki et al. 2019; Moniem 2016; Naghizade and Khoshshima 2018; Naghizade and Saghaei 2020b), comparators (Fakouri-Farid and Andalib 2018; Jile 2020; Seraj et al. 2020), adders and subtractors (Alipour-Banaei and Seif-Dargahi 2017; Hosseinzadeh Sani et al. 2020; Moradi 2019), and switches (Ghadrdan and Mansouri-Birjandi 2017; Jalali Azizpour et al. 2019; Radhouene et al. 2018; Rajasekar et al. 2019).

Various devices incorporating PCRR have been proposed among which are rod ring resonators (Daghooghi et al. 2018; Foroughifar et al. 2021) that find applications in the design of switches and filters. PhC-based all-optical encoders and decoders were also proposed using linear and non-linear functionalities of PhCs (Ghadrdan and Mansouri-Birjandi 2013; Neisy et al. 2018). In these proposed systems, one disadvantage is the tunability of the suggested designs. Nonlinearity in PCRRs which is based on the optical Kerr effect sets a threshold for the magnitude of the incident light. As long as this magnitude is higher than the aforementioned threshold the Kerr effect takes place. However, when the magnitude of

the incident light is higher than the maximum allowed value, it will harm the device (Carr et al. 2004). Daghooghi et al. proposed another optical decoder based on the slow light effect using a nonlinear ring resonator (Daghooghi et al. 2018). In order to increase the light intensity, it is necessary to reduce the speed of light inside the structure. The intensity increase leads to the appearance of nonlinear phenomena such as the optical Kerr effect, which changes the total refractive index. Finally, resonance occurs at the desired wavelength. Its maximum delay is about 6 ps which is one of the drawbacks of this structure. Rostamizadeh et al. (Rostamizadeh et al. 2020) presented an optical decoder based on nonlinear PCRRs. The rise and fall times are 1.5 ps and 0.7 ps, respectively. Mehdizadeh et al. (2017) proposed an optical 2-to-4 binary decoder based on PhC cavities consisting of an enabling port. Despite all advantages of their study, the structure's maximum switching frequency was 20 GHz. The main shortcomings of decoders designed in previous works include low data rate, relatively large area, high input power for the appearance of nonlinear phenomena, and lack of adjustability. To overcome such issues, in this paper, we present an optoelectronic 2-to-4 binary decoder using graphene nanoshells (GNSs) coated on SiO₂ rods in photonic crystal ring resonators. Compared to similar works, the proposed design benefits from using linear rods. Therefore, an increase of the input power to redirect the light emission to the preferred output is not needed. The findings revealed that the decoder has the maximum rise and fall times of 0.8 ps and 0.3 ps, respectively, due to its small area of 200 μm².

In previous works, design parameters such as the radius of the rod and/or the refractive index of the structures were among the factors impacting the resonance frequency of the PhCs. In this work, however, the resonance frequency of the proposed structure depends on the applied voltage to graphene. In addition, the proposed structure in this work benefits from a compact and tunable design that also has a low time response.

The structure of this work is as follows: In Sect. 2, we discuss the GNS characteristics and mathematical formulations, PhC ring resonators, and optoelectronic decoders and their optical behavior. Section 3, covers the design and functionality discussions of the optoelectronic devices and the findings of this work. In Sect. 4, we overview the summary of the findings of this work and present the conclusions.

1.1 Design, model, and methods

1.1.1 Mathematical background

As mentioned earlier in the Introduction, highly tunable, fast, and compact all-optical optoelectronic devices are very desirable. For this reason, in the past decades, graphene which has high electro-optic tunability, optical transmission efficiency, and zero band gap has gained a lot of attention as a 2D material that is ideal for use in fabrications of optoelectronic and plasmonic devices. Enhanced graphene-light interactions are possible due to the strong plasmonic response within a broad range of the spectrum from infrared to terahertz which also results in strong absorption properties. However, in the other parts of the spectrum, such as near-infrared, visible, and UV, a monolayer of graphene has very low absorption in the visible to NIR range and also within the UV region which is due to the absence of the plasmonic response within these regions (Nair et al. 2008).

Tailoring the Fermi energy levels (E_f) of graphene is possible through various methods. One approach is to bias the gate voltage in a substrate-graphene structure set-up. Through this method, one can tune and change the optical characteristics of graphene,

the central resonance frequency of the optoelectronic device of interest, and the quality factor of the system. This method which is in line with the graphene sheet electron flexibility allows for the design and modeling of integrated optoelectronic devices. To this end, various structures have been proposed. Among these are the integration of graphene on insulator substrates made of silicon and silicon dioxide. Here we propose the GNS having a thickness of d which is deposited around the silicon dioxide SiO₂ rod on the SiO₂ substrate. In this proposed structure, the charge carrier density (n_c) could be set by applying the gate voltage (V_g) between the substrate and the GNS. It can be formulated based on Eq. (1) (Shi et al. 2016; Tho et al. 2018).

$$n_c = \frac{V_g \epsilon_0 \epsilon_r}{e r} = V_g C \quad (1)$$

where ϵ_0 and ϵ denote the permittivity of air and the relative permittivity of the substrate of choice, respectively. Further, e represents the electron charge and r is the SiO₂ rod radius and $\frac{\epsilon_0 \epsilon_r}{e r} = C$ where C is the gate capacitance. The chemical potential of graphene is shown as (μ_c) and could be found as follows (Farmani et al. 2017a; Ju et al. 2011):

$$\mu_c = v_f \sqrt{\pi n_c} = v_f \sqrt{\pi V_g C} \quad (2)$$

In Eq. (2), \hbar is the reduced Plank's constant, and the Fermi velocity is represented by v_f . Moreover, the resonance wavelength of the GNS, λ_0 , is obtained through the method described in (Yan et al. 2012):

$$\lambda_0 \approx \frac{2\pi c}{e} \sqrt{\frac{\epsilon_{\text{eff}} \epsilon_0 d \zeta}{E_f}} \quad (3)$$

In Eq. (3), ϵ_{eff} is the effective permittivity of the outer medium of the GNS and is given as $\epsilon_{\text{eff}} = (\epsilon_{\text{SiO}_2} + \epsilon_0)/2$, and d represents the GNS thickness (Farmani et al. 2017b). $\zeta = 3.1$ which is the fitting parameter which is a dimensionless constant. The conductivity δ of a GNS at $T = 300^0$ k for infrared to THz range could be estimated via the formulation given in Eq. (4) (Casiraghi et al. 2007; Naghizade and Saghaei 2020a).

$$\delta \approx \frac{ie^2 E_f}{\pi^2 (\omega + i \tau^{-1})} \quad (4)$$

here τ and ω represent the electron relaxation time and the angular frequency, respectively. Furthermore, the conductivity for N-layer GNS is shown as $N\delta$. Here N denotes the number of GNS layers. In recent works on PhCs, the finite difference time domain method (FDTD) has been suggested to analyze electromagnetic wave propagation in compact optical devices. FDTD can provide a comprehensive solution to Maxwell's equations in a small volume of the PhC of interest (Gedney 2011). In this work, we have used the FDTD method to solve Maxwell's equations and analyze the light propagation in the waveguide of interest. Further, the plane wave expansion (PWE) method is used to calculate the photonic band gap (PBG). In the following equation, the formulation for the optical absorption of graphene is provided

$$A(\lambda) = \frac{4\pi c}{\lambda} n(\lambda) k(\lambda) \int_V |E_l|^2 dV \quad (5)$$

In Eq. (5), c is the speed of light in a vacuum, V stands for the volume of graphene and E_l represents the local electric field. Based on Eq. (5), we could observe that the light absorption is directly proportional to the square of local electric field intensity.

1.2 Optoelectronic decoder and its ring resonator

The 2D PhC proposed in this work has a square type of lattice made of Si and SiO₂ rods. The Si rod has a radius of 118 nm, a lattice constant of $a = 590$ nm, and a refractive index of 3.46 at $\lambda = 1550$ nm. The SiO₂ rod has a 108 nm radius, and a linear refractive index of 1.4. Figure 1 depicts the PBG of the proposed structure. It could be observed that in TM mode, the first PBG is at $0.29 < a/\lambda < 0.4$. This bans wavelengths within the $1439 \text{ nm} < \lambda < 2034$ range from propagation in any direction within the PhC. From the results of Fig. 1, it can be seen that the proposed structure is suitable for working at 1550 nm.

Figure 2 shows the suggested PCRR structure. Its working principle is discussed by Chhipa et. al in (Chhipa et al. 2021). The GNS and SiO₂ defect rods are depicted in red and green colors, respectively. The defect rods are covered by 10 nm thick GNSs. It has a single input port and a dual output port for A and B. A beam of light with a center frequency of 1550 nm is injected into the input port of the waveguide and dropped to the PCRR. The output signal of the PCRR is dependent on the value of GNS chemical potential (μ_c). In Figs. 3a, b, the time-domain light propagation inside the PCRR for two values of μ_c are depicted.

Figure 3a shows that when the μ_c is 0.3 eV, the optical beam cannot enter the resonator and continues the propagation path directly to the output port of B. In this case, the measured power is more than 90%. Figure 3b illustrates that when μ_c is 0.6 eV, the optical beam

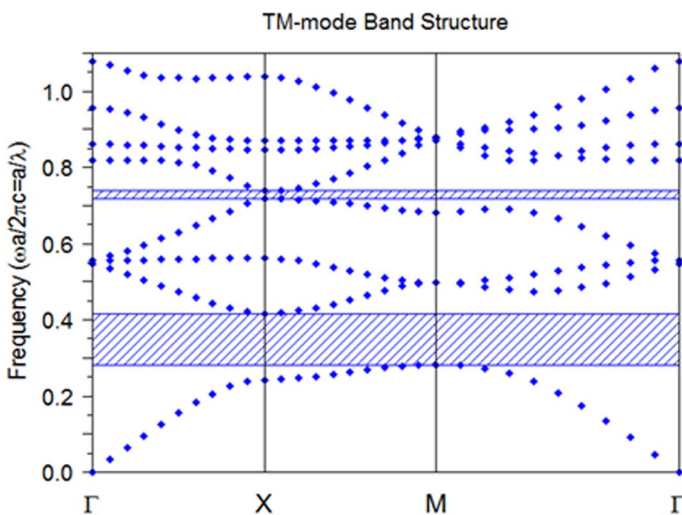


Fig. 1 Fig. 4. The fundamental PhC's band structure diagram in TM mode

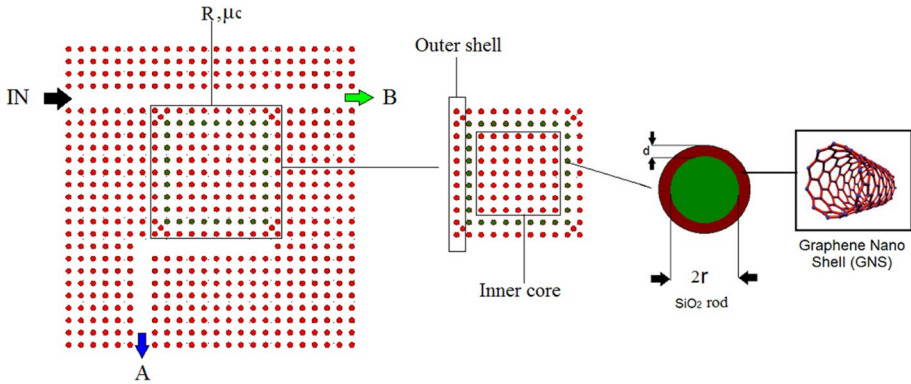


Fig. 2 The schematic of the proposed PhC structure in this work

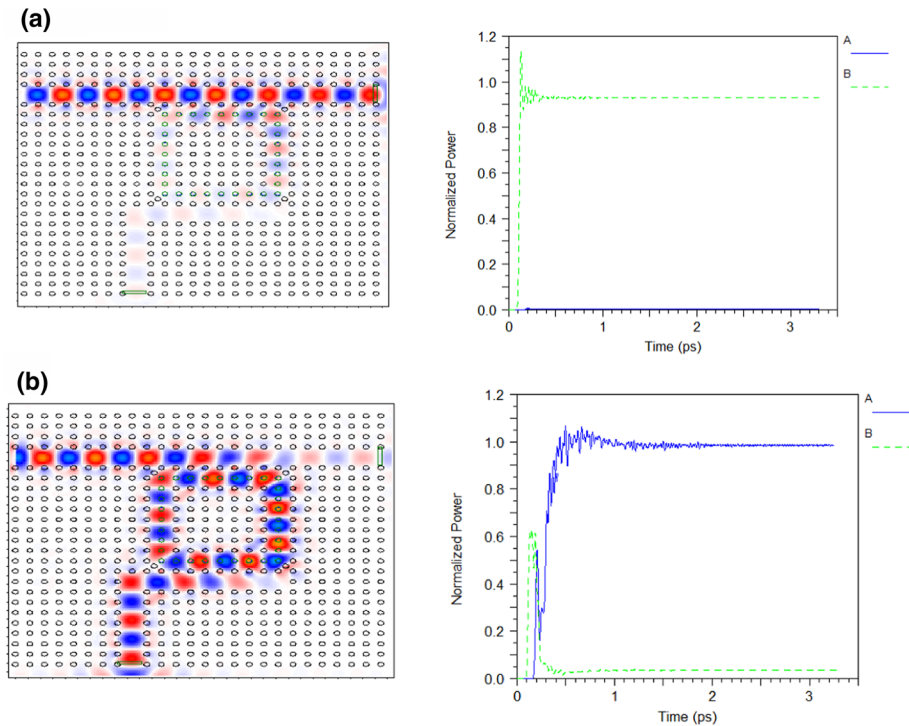


Fig. 3 Light propagation inside the GNS-based PCRR for different values of chemical potential **a** $\mu_c=0.3$ eV and **b** $\mu_c=0.6$ eV

can propagate inside the resonator and is directed to the output port (i.e., Port A). The measured power, in this case, is more than 95%.

As it could be observed in Fig. 4, the suggested optoelectronic 2-to-4 binary decoder is made of multiple waveguides and GNS-based ring resonators in the proposed PhC structure. As depicted in Fig. 4a, E represents the enable port, X and Y display the input ports, and O0, O1, O2, and O3 are the output ports of the decoder. The total size of this

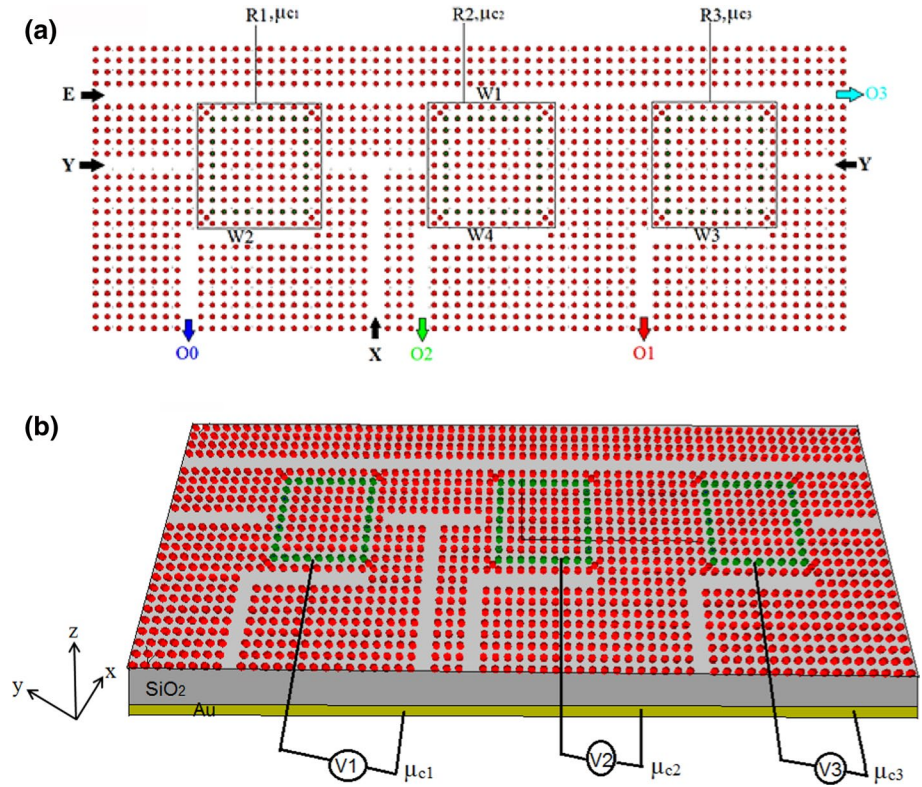


Fig. 4 Schematics of the proposed optoelectronic 2-to-4 binary decoder, **a** top view in XY plane, and **b** the perspective view

miniaturized device is $850 \mu\text{m}^2$. The Y input port, W2 waveguide, and R1 resonator with μ_{c1} form the first switch. The X input port, W4 waveguide, and R2 resonator with μ_{c2} make the second switch. The Y input port, W3 waveguide, and R3 resonator with μ_{c3} also form the third switch. For the sake of clarity, the 3D view of the presented decoder is represented in Fig. 4b, the SiO_2 substrate is shown in grey and is $2 \mu\text{m}$ thick. Gate voltages of V_1 , V_2 , and V_3 are applied to the first, second, and third PCRRs, respectively. This will tune the output states of the decoder by altering the μ_c values in the ring resonators.

2 Simulation and results

In this work, we have used the FDTD method to computationally analyze the light propagation inside the suggested decoder consisting of two input ports of X and Y. The PML boundary conditions were assumed for all boundaries. The mesh size is chosen so fine that all changes in the geometric structure can be applied in the calculations. According to the computational principle, we have 2^2 (2^N , N denotes the number of input ports of the binary decoder) outputs and an optical signal centered at 1550 with an electric field of 1 V/m is injected into every active input port. For all four states of input ports, the computational findings are conferred as follows.

Case #1: In this scenario, input ports X and Y are kept inactive, which means that the applied signal strength is insignificant. We set the μ_1 to 0.6 eV. Since μ_2 and μ_3 are less than 0.6 eV, the optical beam coming from E inside the W1 waveguide will be dropped into W2, and no optical waves travel in the direction of R2 and R3. Thus, O0 will be ON, and the other ports will be OFF in this case (see Fig. 5a). Figure 5b illustrates that the normalized power (the ratio of total output power to input power) at O0 is around 80%; however, the normalized powers at other ports are $< 5\%$. Moreover, for O0, the rise and fall times are around 0.6 ps and 0.1 ps, respectively.

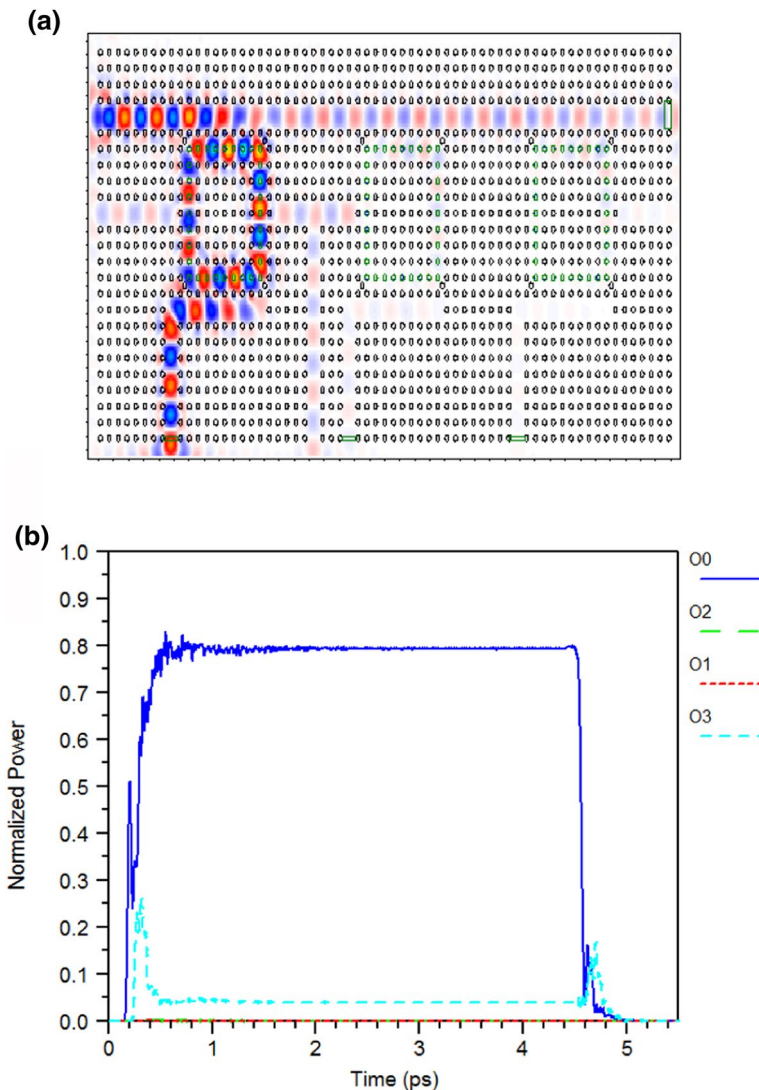


Fig. 5 a The electric field distribution along with b the optical decoder's time response diagram when both X and Y are OFF

Case #2: In this scenario, $X=1$, and $Y=0$, by biasing the V_3 , we set the μ_3 to 0.6 eV. Since μ_1 and μ_2 are less than 0.6 eV, the electromagnetic waves coming from E propagate close to R3 through W1 and drop into W3. Therefore, the O1 output port associated with W3 will be active ($O1=1$), and other output ports remain inactive ($O0=0$, $O2=0$, and $O3=0$). Figure 6a depicts the electric field distribution within the suggested decoder. The time response diagram is represented in Fig. 6b, where the amount of normalized power at port O1 is about 85% while it is less than 3% for other ports. The rise and fall times for O1 are 0.8 ps and 0.3 ps, respectively.

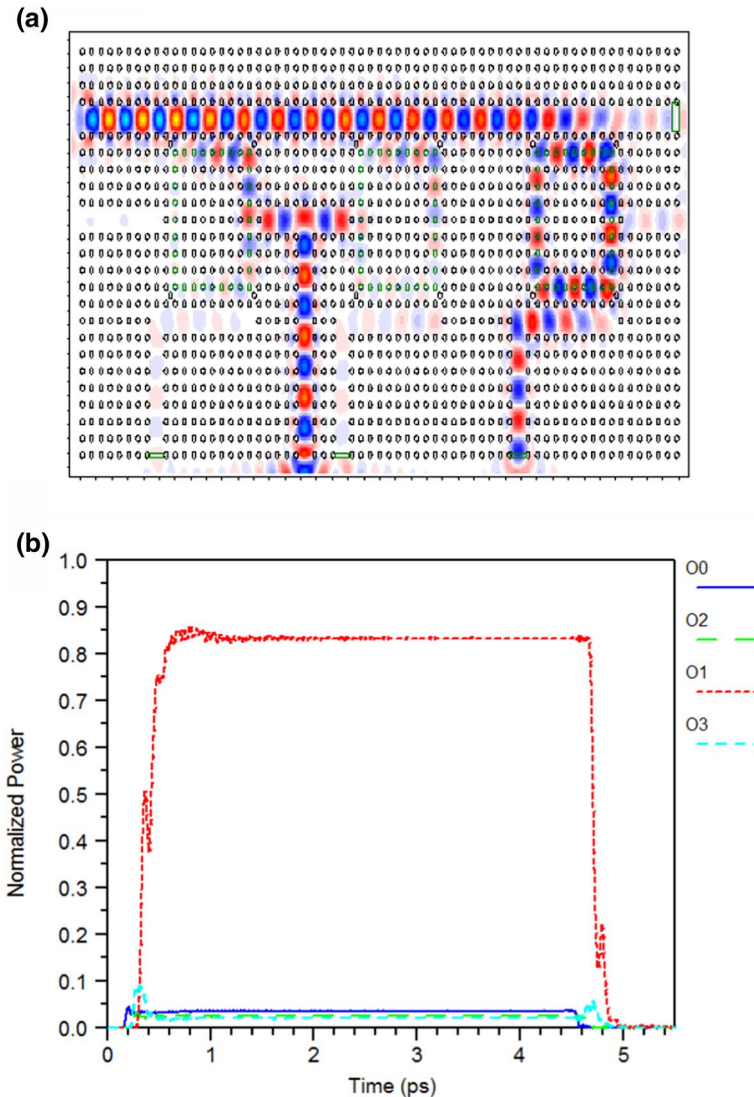


Fig. 6 a The electric field distribution as well as b the optical decoder's time response diagram when $X=1$ and $Y=0$

Case #3: IN this scenario, $X=0$, and $Y=1$, by biasing the V_2 , $\mu_2=0.6$ eV. Since μ_1 and μ_3 are less than 0.6 eV, the light coming from E propagates close to R2 through W1 and drops into W4. Therefore, the O2 output port corresponding to W4 will be active ($O_2=1$), and other output ports remain inactive ($O_0=0$, $O_1=0$, and $O_3=0$). Figure 7a demonstrates the electric field distribution inside the decoder structure. The time response diagram is represented in Fig. 7b, where the amount of normalized power at O2 is about 90% and less than 5% for other ports. The rise and fall times of O_2 are around 0.7 ps and 0.2 ps, respectively.

Case #4: IN this scenario, both input ports X and Y are active, resulting in $X=1$, and $Y=1$. Since μ_1 , μ_2 and μ_3 are less than 0.6 eV, the light propagating from E travels closely to

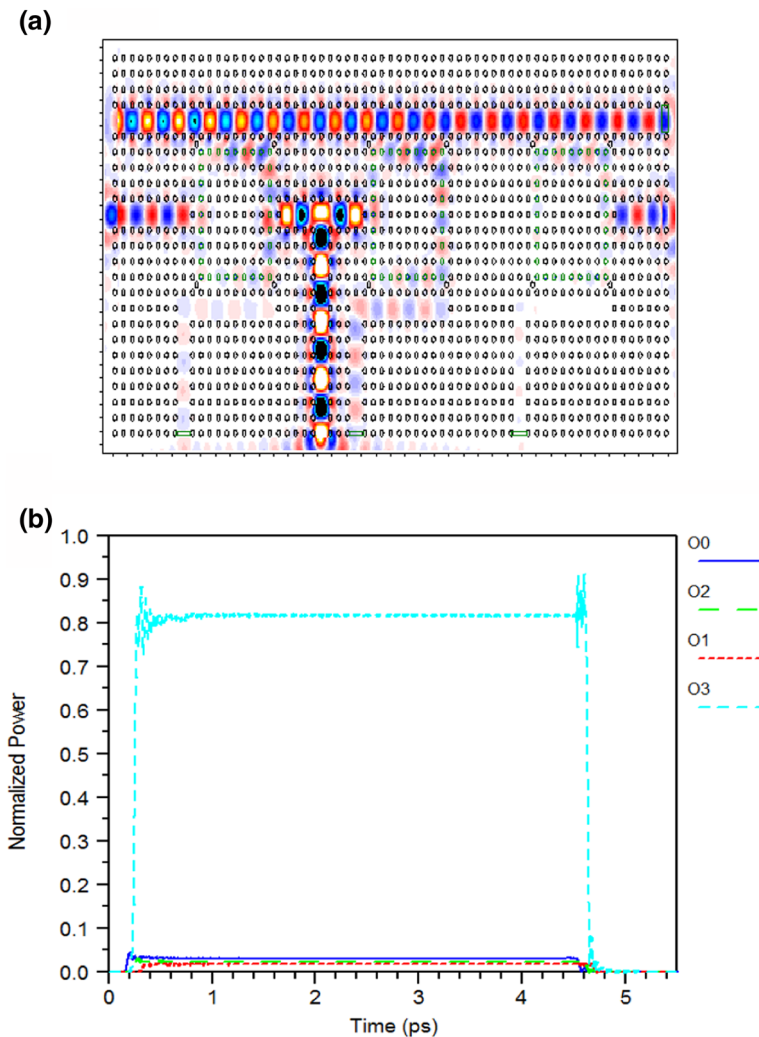


Fig. 7 a The electric field distribution as well as b the optical decoder's time response diagram when $X=0$ and $Y=1$

R1, R2, and R3 through W1. Since the bias voltages of the resonators are below a certain threshold, none of the resonators can absorb the incoming light. As a result, the optical waves traveling from the E port reach O3. Thus, O3 will be active ($O3=1$), and other output ports remain inactive ($O0=0$, $O1=0$, and $O2=0$). Figure 8a demonstrates the electric field distribution inside the proposed decoder. Figure 8b shows the time response diagram where the quantity of normalized power at O3 is around 82% and is less than 3% for other ports. The rise and fall times for O3 are 0.5 ps and 0.15 ps, respectively. Table 1 summarizes the simulation results for the presented structure. The results discussed in this work, confirm that the suggested structure can operate as an optoelectronic 2-to-4 binary decoder. The ON/OFF contrast ratio for each of the outputs can easily be determined by dividing the percentage of logic 1 by the percentage of logic 0. These calculated ratio results are presented in Table 2. For the proposed structure, the worst rise and fall times are about 0.8 ps

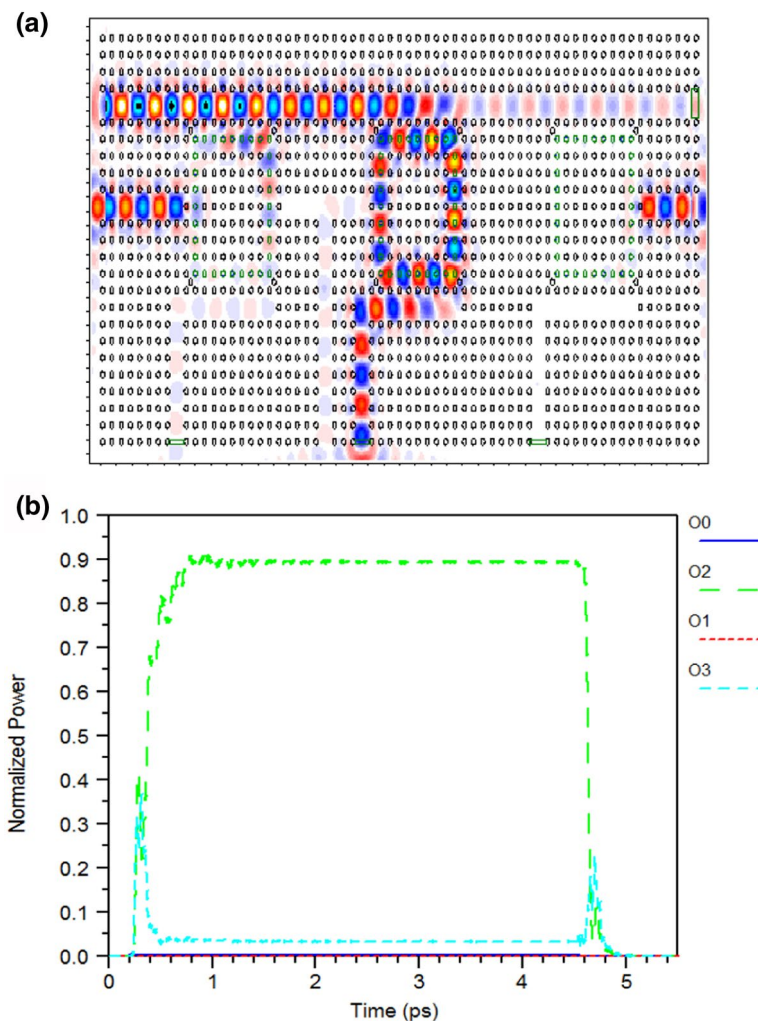


Fig. 8 **a** The electric field distribution as well as **b** the optical decoder's time response diagram when $X=1$ and $Y=1$

Table 1 The input and output states of the decoder

Case	Input		Normalized Outputs (%)				Logic Levels			
	X	Y	O1	O2	O3	O4	O1	O2	O3	O4
#1	0	0	86	2	2	2	1	0	0	0
#2	1	0	4	91	3	4	0	1	0	0
#3	0	1	4	4	90	3	0	0	1	0
#4	1	1	2	2	2	82	0	0	0	1

Table 2 The comparison between the proposed decoder and other structures in recently published papers

Works	Mechanism	Contrast ratio(dB)	Rise time(ps)	Fall time(ps)
Mehdzadeh et al.(2018)	Nonlinear	–	2.5	–
Daghooghi et al. (2018a)	Nonlinear	4.3	6.1	–
Moniem (2015)	linear	–	3.7	6.2
Rostamizadeh et al(2020)	Nonlinear	10.6	1.5	0.7
Askarian (2021)	Nonlinear	7.73	1.2	0.4
This work	Chemical potential of graphene	13.5	0.8	0.3

and 0.3 ps. The ON/OFF contrast ratio for the proposed structure is about 13.5 dB. The comparison of the proposed decoder with other works is listed in Table 2.

3 Conclusion

In this work, we have proposed a new design for a fast and tunable optoelectronic 2-to-4 binary decoder using graphene-coated silica rods in photonic crystal ring resonators. The presented device consisted of three GNS-based ring resonators and several waveguides for input and output ports. Four different states were simulated and discussed for given inputs. Based on the computational findings of this work, it could be observed that the presented decoder is tunable by changing the μc of GNS material of the ring resonator. The maximum rise and fall times were about 0.8 ps and 0.3 ps. The ON/OFF contrast ratio is about 13.5 dB. Compared to previous works published so far, the most important advantages of the presented structure are its lower rise and fall times and tunability. Therefore, it is a proper tool for fast data processing devices.

Author contributions SN: Conceptualization, Data curation, Formal analysis, Funding acquisition, Investigation, Methodology, Software. ADB: Funding acquisition, Validation, Visualization, Roles/Writing—original draft, Writing. HS: Project administration, Resources, Software, Supervision, Validation, Visualization, Writing—review and editing.

Funding This research received no specific grant from any funding agency in the public, commercial, or not-for-profit sectors.

Availability of data and material The data that support the findings of this study are available from the corresponding author upon reasonable request.

Declarations

Competing interests The authors declare no competing interests.

Conflict of interest The authors declare no conflicts of interest.

Ethics approval The ethical issues, including plagiarism, informed consent, misconduct, data fabrication and/or falsification, double publication and/or submission, and redundancy, have been completely observed by the authors.

References

- Alipour-Banaei, H., Jahanara, M., Mehdizadeh, F.: T-shaped channel drop filter based on photonic crystal ring resonator. *Optik (stuttg)*. **125**, 5348–5351 (2014)
- Alipour-Banaei, H., Seif-Dargahi, H.: Photonic crystal based 1-bit full-adder optical circuit by using ring resonators in a nonlinear structure. *Photon. Nanostruct. Fund. Appl.* **24**, 29–34 (2017)
- Alipour-Banaei, H., Serajmohammadi, S., Mehdizadeh, F.: Optical wavelength demultiplexer based on photonic crystal ring resonators. *Photon. Netw. Commun.* **29**, 146–150 (2015a)
- Alipour-Banaei, H., Serajmohammadi, S., Mehdizadeh, F., Andalib, A.: Band gap properties of two-dimensional photonic crystal structures with rectangular lattice. *J. Opt. Commun.* **36**, 109–114 (2015b)
- Andalib, P., Granpayeh, N.: All-optical ultracompact photonic crystal AND gate based on nonlinear ring resonators. *J. Opt. Soc. Am. B.* **26**, 1, 10–16 (2009). <https://doi.org/10.1364/josab.26.000010>
- Askarian, A.: Design and analysis of all optical 2×4 decoder based on kerr effect and beams interference procedure. *Opt Quantum Electron.* **53**, 1–17 (2021)
- Bao, Q., Loh, K.P.: Graphene photonics, plasmonics, and broadband optoelectronic devices. *ACS Nano* **6**, 3677–3694 (2012). <https://doi.org/10.1021/nm300989g>
- Calizo, I., Bao, W., Miao, F., Lau, C.N., Balandin, A.A.: The effect of substrates on the Raman spectrum of graphene: Graphene-on-sapphire and graphene-on-glass. *Appl Phys Lett.* **91**, 201904 (2007). <https://doi.org/10.1063/1.2805024>
- Carr, C.W., Radousky, H.B., Rubenchik, A.M., Feit, M.D., Demos, S.G.: Localized dynamics during laser-induced damage in optical materials. *Phys Rev Lett.* **92**, 87401 (2004). <https://doi.org/10.1103/PhysRevLett.92.087401>
- Casiraghi, C., Hartschuh, A., Lidorikis, E., Qian, H., Harutyunyan, H., Gokus, T., Novoselov, K.S., Ferrari, A.C.: Rayleigh imaging of graphene and graphene layers. *Nano Lett.* **7**, 2711–2717 (2007). <https://doi.org/10.1021/nl071168m>
- Cheraghi, F., Soroosh, M., Akbarizadeh, G.: An ultra-compact all optical full adder based on nonlinear photonic crystal resonant cavities. *Superlattices Microstruct.* **113**, 359–365 (2018). <https://doi.org/10.1016/j.spmi.2017.11.017>
- Chhipa, M.K., Madhav, B.T.P., Robinson, S., Janyani, V., Suthar, B.: Realization of all-optical logic gates using a single design of 2D photonic band gap structure by square ring resonator. *Opt. Eng.* **60**, 075104 (2021)
- Daghooghi, T., Soroosh, M., Ansari-Asl, K.: A low-power all optical decoder based on photonic crystal nonlinear ring resonators. *Optik (stuttg)*. **174**, 400–408 (2018). <https://doi.org/10.1016/j.ijleo.2018.08.090>
- Danaie, M., Kaatuzian, H.: bandwidth improvement for a photonic crystal optical Y-splitter. *J Opt Soc Korea.* **15**, 283–288 (2011)
- Ebnali-Heidari, M., Dehghan, F., Saghaei, H., Koohi-Kamali, F., Moravvej-Farshi, M.K.: Dispersion engineering of photonic crystal fibers by means of fluidic infiltration. *J Mod Opt.* **59**, 1384–1390 (2012). <https://doi.org/10.1080/09500340.2012.715690>
- Ebnali-Heidari, M., Saghaei, H., Koohi-Kamali, F., Naser Moghadasi, M., Moravvej-Farshi, M.K.: Proposal for supercontinuum generation by opto fluidic infiltrated photonic crystal fibers. *IEEE J. Select. Top. Quant. Electron.* **20**, 5, 582–589 (2014). <https://doi.org/10.1109/JSTQE.2014.2307313>

- Fakouri-Farid, V., Andalib, A.: Design and simulation of an all optical photonic crystal-based comparator. *Optik (stuttg)*. **172**, 241–248 (2018). <https://doi.org/10.1016/j.ijleo.2018.06.153>
- Farmani, A., Miri, M., Sheikhi, M.H.: Analytical modeling of highly tunable giant lateral shift in total reflection of light beams from a graphene containing structure. *Opt Commun*. **391**, 68–76 (2017a)
- Farmani, A., Miri, M., Sheikhi, M.H.: Design of a high extinction ratio tunable graphene on white graphene polarizer. *IEEE Photon. Technol. Lett.* **30**, 153–156 (2017b)
- Farmani, A., Soroosh, M., Mozaffari, M.H., Daghooghi, T.: Optical nanosensors for cancer and virus detections. In: *Nanosens Smart Cities*, pp. 419–432. Elsevier (2020)
- Foroughifar, A., Saghaei, H., Veisi, E.: Design and analysis of a novel four-channel optical filter using ring resonators and line defects in photonic crystal microstructure. *Opt Quantum Electron*. **53**, 101 (2021)
- Gedney, S.D.: Introduction to the Finite-Difference time-domain (FDTD) method for electromagnetics. *Synth. Lectures Comput. Electromag.* **27**, 1–250 (2011). <https://doi.org/10.2200/S00316ED1V01Y201012CEM027>
- Ghadrdan, M., Mansouri-Birjandi, M.A.: Concurrent implementation of all-optical half-adder and AND & XOR logic gates based on nonlinear photonic crystal. *Opt Quantum Electron*. **45**, 1027–1036 (2013). <https://doi.org/10.1007/s11082-013-9713-1>
- Ghadrdan, M., Mansouri-Birjandi, M.A.: Low-threshold ultrafast all-optical switch implemented with metallic nanoshells in the photonic crystal ring resonator. *Superlattices Microstruct.* **111**, 789–795 (2017)
- Guo, Y., Zhang, S., Li, J., Li, S., Cheng, T.: A sensor-compatible polarization filter based on photonic crystal fiber with dual-open-ring channel by surface plasmon resonance. *Optik (Stuttg)* **193**, 162868 (2019). <https://doi.org/10.1016/j.ijleo.2019.05.074>
- Haddadan, F., Soroosh, M., Alaei-Sheini, N.: Designing an electro-optical encoder based on photonic crystals using the graphene–Al₂O₃ stacks. *Appl Opt*. **59**, 2179–2185 (2020)
- Hosseinzadeh Sani, M., Ghanbari, A., Saghaei, H.: An ultra-narrowband all-optical filter based on the resonant cavities in rod-based photonic crystal microstructure. *Opt Quantum Electron*. **52**, 295 (2020). <https://doi.org/10.1007/s11082-020-02418-1>
- Hussein, H.M.E., Ali, T.A., Rafat, N.H.: New designs of a complete set of Photonic Crystals logic gates. *Opt Commun*. **411**, 175–181 (2018). <https://doi.org/10.1016/j.optcom.2017.11.043>
- Jalali Azizpour, M.R., Soroosh, M., Dalvand, N., Seifi-Kavian, Y.: All-optical ultra-fast graphene-photonic crystal switch. *Crystals (Basel)*. **9**, 461 (2019)
- Jiang, Y.C., Liu, S. bin, Zhang, H.F., Kong, X.K.: Realization of all optical half-adder based on self-collimated beams by two-dimensional photonic crystals. *Opt Commun*. **348**, 90–94 (2015). Doi: <https://doi.org/10.1016/j.optcom.2015.03.011>
- Jile, H.: Realization of an all-optical comparator using beam interference inside photonic crystal waveguides. *Appl Opt*. **59**, 3714 (2020). <https://doi.org/10.1364/ao.385744>
- Ju, L., Geng, B., Horng, J., Girit, C., Martin, M., Hao, Z., Bechtel, H.A., Liang, X., Zettl, A., Shen, Y.R., Wang, F.: Graphene plasmonics for tunable terahertz metamaterials. *Nat Nanotechnol*. **6**, 630–634 (2011). <https://doi.org/10.1038/nnano.2011.146>
- Liu, Q., Ouyang, Z.B.: All-optical half adder based on cross structures in two-dimensional photonic crystals. *Guangzi Xuebao/acta Photonica Sinica*. **37**, 46–50 (2008). <https://doi.org/10.1364/oe.16.018992>
- Maleki, M.J., Mir, A., Soroosh, M.: Designing an ultra-fast all-optical full-adder based on nonlinear photonic crystal cavities. *Opt Quantum Electron*. **52**, 1–11 (2020)
- Maleki, M.J., Soroosh, M., Mir, A.: Improving the performance of 2-to-4 optical decoders based on photonic crystal structures. *Crystals (Basel)*. **9**, 635 (2019)
- Mansouri-Birjandi, M.A., Tavousi, A., Ghadrdan, M.: Full-optical tunable add/drop filter based on nonlinear photonic crystal ring resonators. *Photonics Nanostruct.* **21**, 44–51 (2016). <https://doi.org/10.1016/j.photonics.2016.06.002>
- Mehdizadeh, F., Soroosh, M., Alipour-Banaei, H.: An optical demultiplexer based on photonic crystal ring resonators. *Optik (stuttg)*. **127**, 8706–8709 (2016). <https://doi.org/10.1016/j.ijleo.2016.06.086>
- Mehdizadeh, F., Soroosh, M., Alipour-Banaei, H.: Proposal for 4-to-2 optical encoder based on photonic crystals. *IET Optoelectron.* **11**, 29–35 (2017). <https://doi.org/10.1049/iet-opt.2016.0022>
- Moniem, T.A.: All-optical digital 4 × 2 encoder based on 2D photonic crystal ring resonators. *J Mod Opt.* **63**, 735–741 (2016). <https://doi.org/10.1080/09500340.2015.1094580>
- Moradi, R.: All optical half subtractor using photonic crystal based nonlinear ring resonators. *Opt Quantum Electron*. **51**, 119 (2019). <https://doi.org/10.1007/s11082-019-1831-y>

- Naghizade, S., Khoshshima, H.: Low input power an all optical 4×2 encoder based on triangular lattice shape photonic crystal. *Journal of Optical Communications*. **1**, 1–8 (2018). <https://doi.org/10.1515/joc-2018-0019>
- Naghizade, S., Saghaei, H.: Tunable graphene-on-insulator band-stop filter at the mid-infrared region. *Opt Quantum Electron*. **52**, 224 (2020a). <https://doi.org/10.1007/s11082-020-02350-4>
- Naghizade, S., Saghaei, H.: A novel design of all-optical 4 to 2 encoder with multiple defects in silica-based photonic crystal fiber. *Optik (Stuttg)*. **222**, 165419 (2020b). <https://doi.org/10.1016/j.ijleo.2020.165419>
- Naghizade, S., Saghaei, H.: A novel design of all-optical full-adder using nonlinear X-shaped photonic crystal resonators. *Opt Quantum Electron*. **53**, 154, 1–13 (2021). <https://doi.org/10.1007/s11082-021-02805-2>
- Nair, R.R., Blake, P., Grigorenko, A.N., Novoselov, K.S., Booth, T.J., Stauber, T., Peres, N.M.R., Geim, A.K.: Fine structure constant defines visual transparency of graphene. *Science*. **320**, 1308 (2008)
- Neisy, M., Soroosh, M., Ansari-Asl, K.: All optical half adder based on photonic crystal resonant cavities. *Photon Netw. Commun*. **35**, 245–250 (2018)
- Radhouene, M., Najjar, M., Chhipa, M.K., Robinson, S., Suthar, B.: Design and analysis a thermo-optic switch based on photonic crystal ring resonator. *Optik (stuttg)*. **172**, 924–929 (2018). <https://doi.org/10.1016/j.ijleo.2018.07.118>
- Rahmani, A., Mehdizadeh, F.: Application of nonlinear PhCRRs in realizing all optical half-adder. *Opt Quantum Electron*. **50**, 30 (2018). <https://doi.org/10.1007/s11082-017-1301-3>
- Rajasekar, R., Parameshwari, K., Robinson, S.: Nano-optical switch based on photonic crystal ring resonator. *Plasmonics* **14**, 1687–1697 (2019)
- Rakhshani, M.R., Mansouri-Birjandi, M.A.: Realization of tunable optical filter by photonic crystal ring resonators. *Optik (stuttg)*. **124**, 5377–5380 (2013). <https://doi.org/10.1016/j.ijleo.2013.03.114>
- Rakhshani, M.R., Mansouri-Birjandi, M.A.: Design and simulation of four-channel wavelength demultiplexer based on photonic crystal circular ring resonators for optical communications. *Journal of Optical Communications*. **35**, 9–15 (2014). <https://doi.org/10.1515/joc-2013-0022>
- Roelkens, G., Brouckaert, J., Taillaert, D., Dumon, P., Bogaerts, W., van Thourhout, D., Baets, R., Nötzel, R., Smit, M.: Integration of InP/InGaAsP photodetectors onto silicon-on-insulator waveguide circuits. *Opt Express*. **13**, 10102 (2005). <https://doi.org/10.1364/opeex.13.010102>
- Rostamizadeh, A., Taghizadeh, M., Jamali, J., Andalib, A.: Application of photonic crystal based nonlinear ring resonators for realizing all optical 3-to-8 decoder. *Journal of Optical Communications*. **52**, 1–10 (2020). <https://doi.org/10.1515/joc-2020-0094>
- Saghaei, H., Zahedi, A., Karimzadeh, R., Parandin, F.: Line defects on photonic crystals for the design of all-optical power splitters and digital logic gates. *Superlattices Microstruct*. **110**, 133–138 (2017). <https://doi.org/10.1016/j.spmi.2017.08.052>
- Sani, M.H., Tabrizi, A.A., Saghaei, H., Karimzadeh, R.: An ultrafast all-optical half adder using nonlinear ring resonators in photonic crystal microstructure. *Opt Quantum Electron*. **52**, 107 (2020). <https://doi.org/10.1007/s11082-020-2233-x>
- Seraj, Z., Soroosh, M., Alaei-Sheini, N.: Ultra-compact ultra-fast 1-bit comparator based on a two-dimensional nonlinear photonic crystal structure. *Appl Opt*. **59**, 811–816 (2020)
- Sharifi, H., Hamidi, S.M., Navi, K.: A new design procedure for all-optical photonic crystal logic gates and functions based on threshold logic. *Opt Commun*. **370**, 231–238 (2016)
- Shi, B., Cai, W., Zhang, X., Xiang, Y., Zhan, Y., Geng, J., Ren, M., Xu, J.: Tunable band-stop filters for graphene plasmons based on periodically modulated graphene. *Sci Rep*. **6**, 1–7 (2016)
- Song, K.S., Williams, R.T.: Silicon Dioxide. In: *Handbook of optical constants of solids*. pp. 270–299. Elsevier (1993)
- Sun, Z., Martinez, A., Wang, F.: Optical modulators with 2D layered materials. *Nat Photonics*. **10**, 227–238 (2016). <https://doi.org/10.1038/nphoton.2016.15>
- Tavousi, A., Mansouri-Birjandi, M.A., Ghadrddan, M., Ranjbar-Torkamani, M.: Application of photonic crystal ring resonator nonlinear response for full-optical tunable add–drop filtering. *Photon Netw. Commun*. **34**, 131–139 (2017)
- Tho, N.H., Thy, T.T.M., Dat, P.T., Minh, V.C., Sang, N.X.: Physical Adsorption and photocatalytic activity of titanium dioxide nanotube and graphene oxide composite. *VNU Journal of Science: Natural Sciences and Technology*. **34**, (2018)
- Vali-Nasab, A.M., Mir, A., Talebzadeh, R.: Design and simulation of an all optical full-adder based on photonic crystals. *Opt Quantum Electron*. **51**, 241–248 (2019). <https://doi.org/10.1007/s11082-019-1881-1>
- Wabnitz, S., Eggleton, B.J.: All-optical signal processing. *Data Communication and Storage Applications*. (2015)

- Yablonovitch, E.: Photonic band-gap structures. *Journal of the Optical Society of America B*. **10**, 283 (1993). Doi: <https://doi.org/10.1364/josab.10.000283>
- Yan, H., Li, X., Chandra, B., Tulevski, G., Wu, Y., Freitag, M., Zhu, W., Avouris, P., Xia, F.: Tunable infrared plasmonic devices using graphene/insulator stacks. *Nat Nanotechnol*. **7**, 330–334 (2012). <https://doi.org/10.1038/nnano.2012.59>
- Younis, R.M., Areed, N.F.F., Obayya, S.S.A.: Fully integrated and and or optical logic gates. *IEEE Photonics Technol. Lett*. **26**, 1900–1903 (2014). <https://doi.org/10.1109/LPT.2014.2340435>

Publisher's Note Springer Nature remains neutral with regard to jurisdictional claims in published maps and institutional affiliations.

Springer Nature or its licensor holds exclusive rights to this article under a publishing agreement with the author(s) or other rightsholder(s); author self-archiving of the accepted manuscript version of this article is solely governed by the terms of such publishing agreement and applicable law.